Vibration Analysis of Cryogenically Cooled Accelerating Structures

A. Dhar, D. T. Palmer, M. Boyce, R. Conley, Z. George,
V. Borzenets, A. Haase, E. A. Nanni

June 4, 2024

The Cool Copper Collider (C^3) represents a novel path for achieving a future collider within the near future. Its conceptual design pushes the limits of NCRF technology, through the use of both distributed coupling and cryogenically cooled structures. These accelerating structures are cooled via liquid nitrogen vaporization, which can generate minute displacements to the structure's alignment. Characterizing sources of misalignment from external vibrations is a crucial process for this accelerator's design. In order to accurately characterize these displacements, we validated techniques for measuring displacement of a structure immersed in liquid nitrogen. We used a prototype C^3 structure with a hollow dielectric rod threaded with resistive molybdenum wires inserted along the beam pipe running the full length of the structure. Displacement measurements were then conducted as the dissipated power was slowly increased up to 2000 W of heat. Based on accelerometer data, we found that as heater power is increased, significant displacement around 40 Hz, 150 Hz, and 300 Hz would increase as well. None of these peaks are of major concern, since the 40 Hz peak can be corrected for with beam based feedback, while the other peaks were significantly lower in magnitude compared to lower frequency perturbations. These initial experiments were the first step in understanding the types of perturbations that liquid nitrogen bubbling can induce on a submerged accelerating structure due to RF heating. These initial results show displacements of less than 1 μm when up to 2000 W is dissipated within a meter-long copper structure.

Introduction

One of the primary challenges with state of the art normal conducting RF (NCRF) technology is reducing the rate of breakdowns in accelerating structures. It has been observed that breakdowns can be reduced by limiting the peak surfaced electric fields, magnetic fields and Poynting vector in the accelerating cavity [1]. In addition, recent

work has shown that the breakdown rate for an accelerating structure operating at a given gradient can be significantly reduced by cooling it down to 77 K, or liquid nitrogen temperatures [2]. This reduction in temperature also increases the conductivity of the copper, thereby increasing the quality factor, reducing pulsed heating, and increasing efficiency of the accelerating structure [3]. This cryogenic operation not only provides the possibility of reaching higher acceleration gradients with NCRF, but also reduces the power requirements from RF sources, which is a major cost driver and technical challenge for accelerators.

However, the dissipated heat within an accelerating structure needs to be constantly removed to maintain these temperatures. This can done via convective cooling or at the boiling point of liquid nitrogen, where heat is removed via vaporization. Vaporizing liquid nitrogen along the surface will create a turbulent two-phase layer with liquid and gaseous nitrogen bubbles, which in turn can transfer momentum to the linac resulting in minute displacements on the linac. This occurs within the nucleate boiling regime, with an expected temperature rise of $\sim$2 K [4]. Characterizing these displacements is a vital task to understanding how to handle beam alignment and maintain precision while operating any cryogenically cooled accelerating structure.

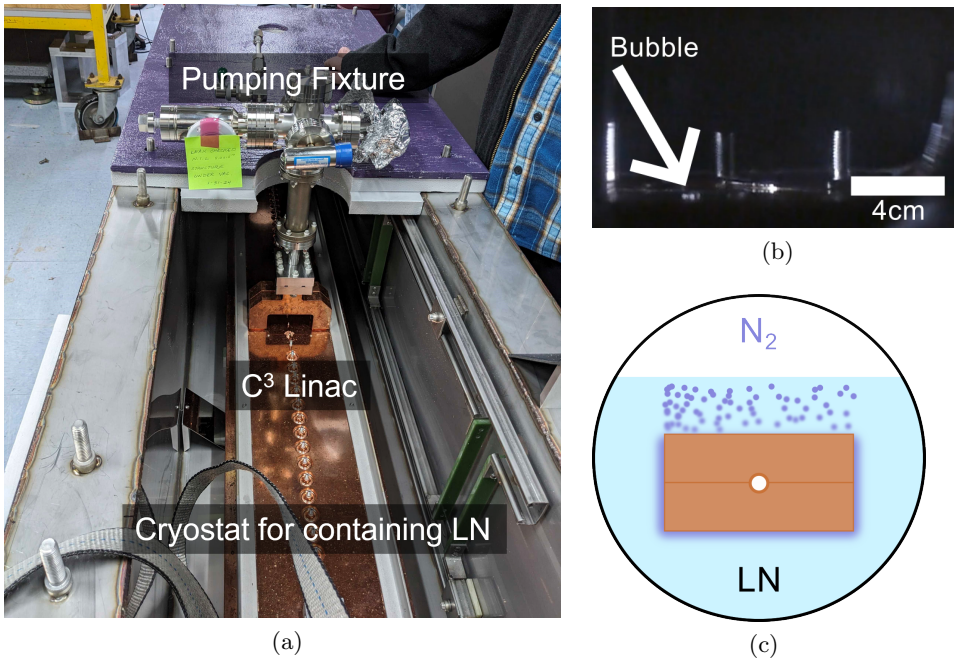

(a) (b) (c)

Figure 1: (a) Picture of the prototype C^3 structure placed within the test cryostat, with pumping fixture attached to maintain vacuum inside. (b) Photograph of the underside of the structure during heating, with evidence of bubble formation. (c) Schematic of how these bubbles (purple) flow around the underside of the copper structure, eventually finding a path to rise upward.

The Cool Copper Collider (C^3) represents the most challenging application of this technology, and a novel path for achieving a future collider within the near future [5, 6]. Its conceptual design pushes the limits of NCRF technology, through the use of both distributed coupling and cryogenically cooled structures. Distributed coupling uses unique waveguide and coupler designs to power each cavity individually [7]. This in turn allows the cavity geometry to be optimized for shunt impedance, resulting in more efficient structures generating an equivalent gradient. Combining these technologies results in a collider that could reach gradients over 120 MV/m and center of mass energy over 500 GeV within an 8 km footprint. As a benchmark for our measurements, the operational parameters and vibration tolerances for the C^3 main linac were considered [8].

Background

Characterizing sources of misalignment from external vibrations is a crucial process for any accelerator design [9, 10]. Depending the specific frequencies of these vibrations, the relevant transfer functions of the mechanical supports can be designed to minimize their impact on the luminosity [11, 12]. Some sources of vibrations, such as those from seismic disturbances (<0.25 Hz) and machinery in the accelerator tunnel (>1 Hz), can be compensated for with inter-bunch train beam feedback [13]. If the beam is used to sample the alignment through beam position monitors, this correction can be done up to bunch train repetition rate, which can be anywhere from 10 to 120 Hz.

The total contribution of these vibrations, within the frequencies of interest, needs to remain within certain tolerances in order to maintain the beam emittance required for a collider's target luminosity. For example, the displacement tolerances for the CLIC accelerating structures in the main linac are 1.4 μm vertically and 8 μm laterally [14]. This is defined as the expected displacement above 10 Hz, which cannot be easily corrected for with beam-based feedback. The primary source of such displacements is cooling machinery, whether they be water cooling or cryogenic cooling. Based on previous studies for NLC and LCLS-II, we can expect the contributions from water cooling to be around 0.5 μm, while liquid helium compressors contribute displacements of around 1 μm to the main linac [15, 16].

Experimental Setup

In order to accurately characterize these displacements, a critical first step was to validate techniques for measuring displacement of a structure immersed in liquid nitrogen. As a first approximation, we used a prototype C^3 structure within which was placed a hollow dielectric rod threaded with molybdenum wires. The power supplies producing a current in the wires could produce up to 2000 W of dissipated heat within the structure. For comparison, the maximum expected dissipated power from RF heating for a single C^3 accelerating structure is 2500 W [6]. The RF heat is dissipated uniformly in each cavity along the length of the accelerating structure, with the majority of the heat deposited at the large radius extents where there is a strong magnetic field. This heater wire was

placed along the center of the structure to approximate this heating profile. In order to prevent the molybdenum heater from reaching its melting point (2900 K), helium gas was introduced to the vacuum environment up to 6 torr. The additional helium gas would allow heat to be carried away via a combination of radiative dissipation and convection, thereby lowering the required wire temperature for dissipating a given amount of heat.

(a) (b)

Figure 2: (a) Laser micrometer mounted outside cryostat along with a reference accelerometer to measure displacement in the Y direction. Automatic liquid nitrogen fill system and data collection in shown on the right. (b) Picture of accelerometers mounted to structure via a aluminum block. The respective axis is labeled for each uni-axial accelerometer.

This entire apparatus was contained within a foam insulated cryostat at atmospheric pressure with an automatic liquid nitrogen filling system. This allowed the structure to remain submerged in liquid nitrogen for extended periods of time unattended, allowing for several rounds of measurements. This cryostat was also mounted onto an optical table with air suspension, so as to decouple any environmental vibrations from the experiment, as shown in Figure 2a.

Once immersed in liquid nitrogen, displacement measurements were conducted as the dissipated power was slowly increased up to 2000 W of heat. The wire temperature could be estimated from the measured resistance across it. Helium gas would be added into the vacuum when this temperature approached 2000 K to bring it back down. The goal with these measurements was to discern a trend in total displacement within the C^3 accelerating structure that is proportional to dissipated heating power. In order to measure these displacements, uni-axial accelerometers were attached to the structure directly as shown in Figure 2b. Each of these accelerometers would be read out over 5 minutes at 6250 samples per second, allowing frequency information up to 3 kHz to be measured. As an independent validation of these accelerometer measurements, a laser micrometer was also used exclusively in the Y-axis, which was expected to have the greatest displacement. This laser micrometer would be readout after 5 seconds of

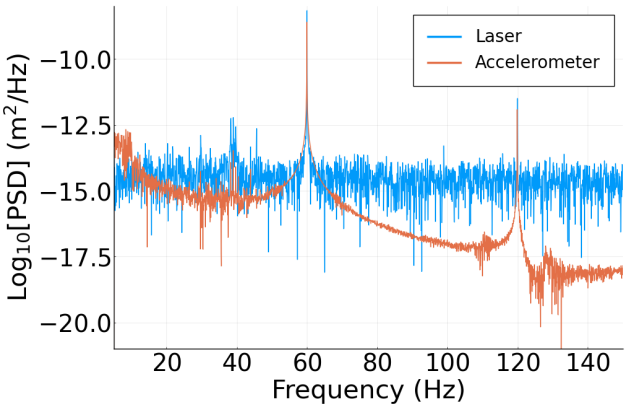

Figure 3: PSD of Y displacement for both laser and accelerometer when calibrated against a piezoelectric transducer running at 60 Hz. As expected the harmonic peaks coincide for both sensors, however the sensitivity of the laser diode is limited to 2-3 μm across this frequency range.

data collection, with sampling up to 10 kHz. A direct calibration between the laser micrometer and accelerometer was done by generating a controlled displacement with a piezoelectric transducer at varying frequencies, as shown in Figure 3.

Analysis Methods

It is important to understand how displacements in a copper accelerating structure as a function of frequency will impact electron beam performance. This is because during operation, the C^3 linac will have a repetition rate of 120 Hz, so displacements that are around that frequency or lower are of greatest concern. However displacements at sufficiently low frequencies (<10 Hz) could be corrected for using beam-based feedback from bunch to bunch. This feedback could directly be fed into the piezoelectric actuators on each raft, which are expected to have a range of $\pm 20\,\mu$m at 80 K up to 1 kHz. In theory this feedback could be extended up to half of the repetition rate (60 Hz) when sampling alignment with the beam position monitors, but for the purposes of this study we chose to focus on displacements between 10 Hz and 300 Hz. Higher frequency feedback could be possible if it were measured by other means, such as a Rasnik alignment system which uses diffraction zone plates for extremely precise alignment features below 1 μm [17].

A common method for analyzing and identifying sources of vibrations is by using the power spectral density (PSD) of the vibration measurement, which is defined as

$$S_x(f) = |x(f)|^2/df, \tag{1}$$

where $x(f)$ is the Fourier transform of the vibrational displacement measurement, and df is the width of the frequency bin [9]. The RMS displacement above a specific frequency

can then be determined by

$$x_{rms}(f_{min}) = \sqrt{\int_{f_{min}}^{\infty} S_x(f)df}, \tag{2}$$

which is helpful when trying to identify displacements above a known low frequency limits that can corrected for during operation. Our accelerometer measurements were broken up into 5 second samples, so df =0.2 Hz, meaning the PSD for a 1 μm displacement would be 5×10^{-12} m^2/Hz.

Processing the accelerometer data required careful analysis, as double integrating acceleration into displacement can often compound existing measurement error. To account for this, the 5 minute data set was broken up into 5 second intervals. This acceleration information is then filtered in frequency space, removing anything below 5 Hz and above 300 Hz so as to remove any slowly varying measurement drift or high frequency noise. This filtered data is then integrated into velocity using a trapezoidal integral. These filtering and integration steps were repeated to transform from velocity into displacement, giving a final measurement that can be analyzed in both time and frequency domains.

Results and Discussion

As a first test, it was important to identify the self-resonance of the assembly, as this frequency is most likely to be excited from the stochastic bubbling. This was identified through a series of impulse tests, where a strong impulse was applied to the table while the structure was immersed in liquid nitrogen, and the induced ringing was analyzed to identify self-resonant frequencies. A strong response in the Y direction around 14 Hz was consistently identified, as shown in Figure 4a, and was taken to be the self-resonance of the assembly. We also verified that adding Helium (up to 6 torr) into the vacuum system did not significantly affect the measured displacements for a given dissipated power level, as shown in Figure 4b, allowing us to make direct comparisons between all of our measurements with and without helium.

Looking at the processed accelerometer data, we found that as heater power is increased, a significant contribution to X displacement rose around 40 Hz, as well as 300 Hz, as shown in Figure 5a. Neither of these peaks are of major concern, since the 40 Hz peak can be corrected for with beam based feedback, while the 300 Hz peak is significantly lower in magnitude compared to lower frequency perturbations in the 40 Hz to 120 Hz range. This 300 Hz peak is also reflected in the Y displacement, as shown in Figure 5b, but is still well below the threshold of concern. We also find the RMS displacement in both the X and Y directions to be less than 1 μm, as measured by the accelerometers and shown in Figure 6.

As expected the displacement in both transverse directions increases as the dissipated power within the structure increases. The variance in these measurements stems from the calibration between the accelerometers and the laser micrometer. However even

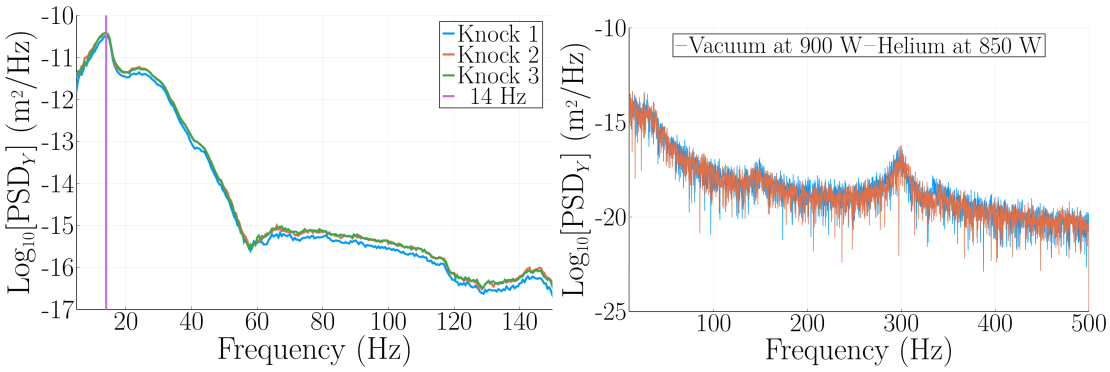

(a) (b)

Figure 4: (a) PSD of Y displacement data from 3 successive knocks perturbing the structure. Each knock sees a peak around 14 Hz, which is likely the self-resonance of the structure. (b) PSD of displacement in the Y direction comparing conditions at vacuum versus using up to 6 torr of helium. Although the heater wire temperature is lower with helium inside, for the same effective heating the PSD is comparable.

when taking these into account, the magnitude of the displacement is well below the noise floor of the laser micrometer, so we can only rely on the accelerometer for these measurements.

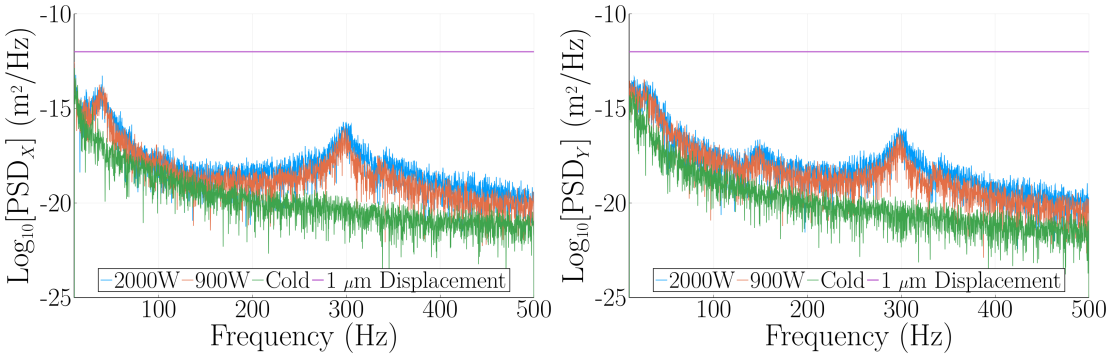

(a) (b)

Figure 5: (a) PSD of displacement data from the X accelerometer, showing peaks around 40 Hz and 300 Hz. For reference the baseline of 1 μm displacement in PSD is shown as well (pink). (b) PSD of displacement data from the Y accelerometer showing a similar rise in displacement as a function of applied power.

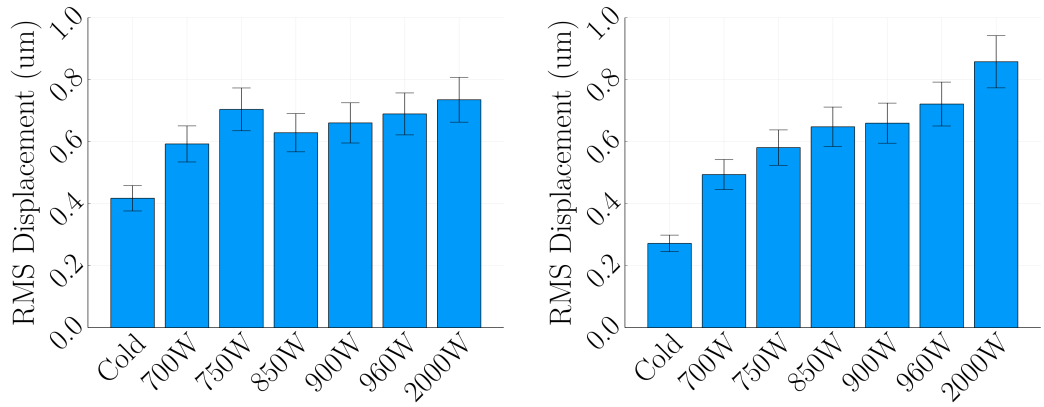

(a) X Displacement (b) Y Displacement

Figure 6: RMS values of displacement integrated from 10 Hz up to 500 Hz using Eq 2 to represent the displacements seen by an accelerated beam. As expected the overall displacement in Y increases with applied power, though the displacement in X might be tapering out. The Z measurements were negligible compared to these two axes.

Conclusion

In conclusion, these initial experiments were the first step in understanding the types of perturbations that liquid nitrogen bubbling can induce on a submerged accelerating structure due to RF heating. These initial results show displacement less than 1 μm when up to 2000 W is dissipated within a meter-long copper structure. While we were able to

observe some visual disturbance in the nitrogen liquid gas interface, the next stage of experiments will focus on resolving clearer images of the bubble formation and cavitation process. This will allow for a more accurate simulation of the expected displacements, and help optimize design of future cryogenic accelerating structures to minimize their contribution to misalignment.

References

[1] A. Grudiev, S. Calatroni, and W. Wuensch. "New local field quantity describing the high gradient limit of accelerating structures". In: *Phys. Rev. ST Accel. Beams* 12 (2009). [Erratum: Phys.Rev.ST Accel.Beams 14, 099902 (2011)], p. 102001. DOI: 10.1103/PhysRevSTAB.12.102001.

[2] Mamdouh Nasr et al. "Experimental demonstration of particle acceleration with normal conducting accelerating structure at cryogenic temperature". In: *Phys. Rev. Accel. Beams* 24 (9 2021), p. 093201. DOI: 10.1103/PhysRevAccelBeams.24.093201. URL: https://link.aps.org/doi/10.1103/PhysRevAccelBeams.24.093201.

[3] A. D. Cahill et al. "High gradient experiments with X -band cryogenic copper accelerating cavities". In: *Phys. Rev. Accel. Beams* 21.10 (2018), p. 102002. DOI: 10.1103/PhysRevAccelBeams.21.102002.

[4] Emilio A. Nanni et al. "C^3 Demonstration Research and Development Plan". In: *Snowmass 2021*. Mar. 2022. arXiv: 2203.09076 [physics.acc-ph].

[5] Karl L. Bane et al. "An Advanced NCRF Linac Concept for a High Energy e^+e^- Linear Collider". In: (July 2018). arXiv: 1807.10195 [physics.acc-ph].

[6] Caterina Vernieri et al. "A "Cool" route to the Higgs boson and beyond. The Cool Copper Collider". In: *Journal of Instrumentation* 18.07 (2023), P07053. DOI: 10.1088/1748-0221/18/07/P07053. URL: https://dx.doi.org/10.1088/1748-0221/18/07/P07053.

[7] Sami Tantawi et al. "Design and demonstration of a distributed-coupling linear accelerator structure". In: *Phys. Rev. Accel. Beams* 23 (9 2020), p. 092001. DOI: 10.1103/PhysRevAccelBeams.23.092001. URL: https://link.aps.org/doi/10.1103/PhysRevAccelBeams.23.092001.

[8] W. H. Tan et al. "Multi-bunch beam dynamics studies for the C3 main linac". English. In: *Proc. 15th International Particle Accelerator Conference* (Nashville, TN). IPAC'24 - 15th International Particle Accelerator Conference 15. JACoW Publishing, Geneva, Switzerland, May 2024, pp. 979–982. ISBN: 978-3-95450-247-9. DOI: 10.18429/JACoW-IPAC2024-TUPC03. URL: https://indico.jacow.org/event/63/contributions/3790.

[9] Maurizio Serluca et al. "Vibration and luminosity frequency analysis of the SuperKEKB collider". In: *Nuclear Instruments and Methods in Physics Research Section A: Accelerators, Spectrometers, Detectors and Associated Equipment* 1025 (2022), p. 166123. ISSN: 0168-9002. DOI: https://doi.org/10.1016/j.nima.2021.166123. URL: https://www.sciencedirect.com/science/article/pii/S016890022101010X.

[10] Tessa K. Charles et al. "Alignment and stability challenges for FCC-ee". In: *EPJ Techniques and Instrumentation* 10.1 (2023), p. 8. ISSN: 2195-7045. DOI: 10.1140/epjti/s40485-023-00096-3. URL: https://doi.org/10.1140/epjti/s40485-023-00096-3.

[11] F. Asiri, F. Le Pimpec, and A. Seryi. "Study of near-field vibration sources for the NLC linac components". In: *Proceedings of the 2003 Particle Accelerator Conference*. Vol. 4. 2003, 2748–2750 vol.4. DOI: 10.1109/PAC.2003.1289254.

[12] M. Schaumann et al. "The effect of ground motion on the LHC and HL-LHC beam orbit". In: *Nuclear Instruments and Methods in Physics Research Section A: Accelerators, Spectrometers, Detectors and Associated Equipment* 1055 (2023), p. 168495. ISSN: 0168-9002. DOI: https://doi.org/10.1016/j.nima.2023.168495. URL: https://www.sciencedirect.com/science/article/pii/S0168900223004850.

[13] D. Tshilumba et al. "Budgeting and control of the mechanical noise in the International Linear Collider final focus system". In: *Phys. Rev. ST Accel. Beams* 17 (6 2014), p. 062801. DOI: 10.1103/PhysRevSTAB.17.062801. URL: https://link.aps.org/doi/10.1103/PhysRevSTAB.17.062801.

[14] Matthew Capstick et al. "Design and optimisation of the Compact Linear Collider main LINAC module for micron-level stability and alignment". In: *Nuclear Instruments and Methods in Physics Research Section A: Accelerators, Spectrometers, Detectors and Associated Equipment* 1038 (2022), p. 166834. ISSN: 0168-9002. DOI: https://doi.org/10.1016/j.nima.2022.166834. URL: https://www.sciencedirect.com/science/article/pii/S0168900222003138.

[15] Frederic Le Pimpec. "Vibrational Stability of NLC Linac accelerating structure". In: (Sept. 2002). DOI: 10.2172/801820. URL: https://www.osti.gov/biblio/801820.

[16] G.L Gassner and Chris Adolphsen. *LCLS-II Cryogenic FacilityCompressor Vibration Assessment*. Tech. rep. SLAC, 2015.

[17] Harry van der Graaf et al. *The alignment of the C3 Accelerator Structures with the Rasnik alignment system*. 2023. arXiv: 2307.07981 [physics.acc-ph].